Critical phenomena of water bridges in nanoasperity contacts

Mingyan He, Amy Szuchmacher Blum, D. Eric Aston, Cynthia Buenviaje, and René M. Overney[a)]
Department of Chemical Engineering, University of Washington, Seattle, Washington 98195

Reto Luginbühl
Department of Bioengineering, University of Washington, Seattle, Washington 98195

(Received 11 August 2000; accepted 18 October 2000)

This article discusses capillary forces measured by scanning force microscopy (SFM), which, as recently reported, show a discontinuous behavior at a low relative humidity between 20% and 40% depending on the solid surfaces. A capillary force discontinuity is very interesting in terms of a possible phase change or restructuring transition of bulk water in the interfacial solid–liquid region. Unfortunately, we have found that SFM measurements show an inherent weakness in the determination of the origin of the forces that are obtained during pull-off measurements. This article critically discusses the origin of the adhesive interactions as a function of relative humidity with chemically modified probing surfaces. Our measurements indicate that force discontinuities in pull-off measurements are strongly affected by the inability of the liquid to form capillary necks below a critical threshold in relative humidity. In the course of this article, we will discuss roughness effects on capillary forces and provide a modified capillary force equation for asperity nanocontacts. © *2001 American Institute of Physics.* [DOI: 10.1063/1.1331298]

INTRODUCTION

The possibility of structural changes in thin water films on surfaces has been repeatedly raised, since mechanical studies on nanometer confined water films were employed by surface forces apparatus (SFA)[1–4] and scanning force microscopy (SFM).[5–15] In SFM measurements, capillary forces have been the focus of many studies due to their dominance in the effective applied load in a humid environment.[6,10,12,14,16,17] Capillary neck formation between two surfaces results from the self-association of water and the strong adhesive properties of water towards the surface. This formation has been extensively studied on both the macroscale and microscale.[5,18–24] The molecular self-association in unfrozen bulk water, also referred to as *structured water*, forms a three-dimensional hydrogen-bonded network that is very important in biological systems and processes.[25] A phenomenon opposing this self-association is the thermodynamic driving force that causes spreading on high energy (hydrophilic) surfaces. The adhesive interaction strength between a surface and a water film can be as high as the cohesive energy density of water (0.1456 N/m).[25] Considering such strong interfacial interactions, it is reasonable to assume that the self-association of water might be hindered within a boundary layer at the wetted surface. If it exists at all, the structurally distorted boundary layer is expected to be only a few monolayers thick due to the short range of the interactions. Recently, Parrinello and co-workers suggested a theoretical ice-like structure for water on the highly polar crystalline surface of mica.[13]

Salmeron and co-workers suggested that water, condensed from water vapor at room temperature on mica, forms a partially developed monolayer of an ice-like phase.[9] Their interpretation was based on results obtained by sum–frequency generation (SFG) vibrational spectroscopy and scanning polarization force microscopy. Thus, they concluded that with decreasing humidity the ice-like water monolayer, which is formed around 90% relative humidity (RH), breaks into islands until the water coverage is too low (20% RH) to provide enough SFG signal. Other findings that were based on SFM pull-off force measurements offer divergent interpretations.[7,8,20] For instance, force instabilities observed around 20%–30% RH were interpreted as a strongly bound water layer.[6]

In this article, we critically discuss the SFM pull-off force approach as a tool for determining structural changes in water films on solid sample surfaces. We describe the different adhesive interaction force regimes from low to high RH.

CAPILLARY FORCE TRANSITION

The origin for capillary interactions is the capillary neck. Structured bulk water strongly affects the surface tension of the water–air interface, i.e., the mechanical properties of neck sidewalls. At the water–solid interface, the water experiences surface adhesion that competes with the molecular self-association of bulk water. At sufficiently low humidity, i.e., in a spatially confined liquid film of only a few molecular layers, it can be expected that the interfacial interaction is powerful enough to distort the bulk structure.

Salmeron and co-workers employed SFM adhesion measurements on mica surfaces as a function of the humidity and noticed that there are three distinct force regimes as illustrated in Fig. 1 (regimes I, II, and III). In regime I, the measured pull-off forces are depressed if compared to the forces

[a)]Author to whom correspondence should be addressed.

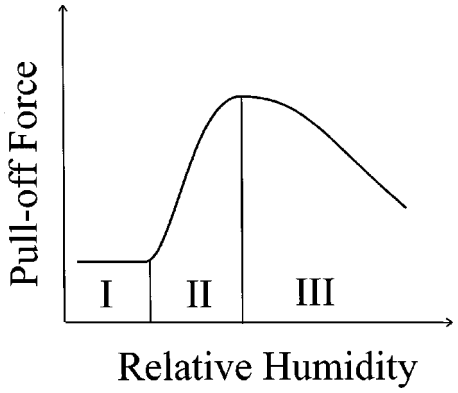

FIG. 1. Generic sketch of the functional relationship between the pull-off force and the relative humidity. Regimes I, II, and III represent the van der Waals regime, mixed van der Waals–capillary regime, and capillary regime decreased by repulsive forces, respectively.

in regimes II and III. The qualitative force behavior from regime I to II has been confirmed by others with hydrophilic SFM tips on mica.[10,14] In order to reflect on the possibility that the qualitative transition behavior resembles a structural change of water, it has first to be discussed on how a structural change would affect the observable force.

Typically, the capillary force of bulk water is estimated by the following equation, assuming a sphere–plane geometry (Fig. 2),

$$F_{\mathrm{cap}}^{R\gg d}=4\pi R\gamma\cos\theta, \tag{1}$$

where R is the radius of the sphere, d the length of $\overline{PQ}$, γ the liquid surface tension, and θ the meniscus contact angle.[26] A more elaborate equation for nanocontact (i.e., $R\sim d$) can be found in the Appendix.

Note that the capillary force described by Eq. (1) is only dependent on the surface tension of bulk water and the contact angle θ, but is independent of the solid–liquid and solid–solid interaction parameters. Equation (1) predicts a gradual change in the capillary force with the meniscus contact angle. For constant γ, this equation does not explain the force transition experimentally observed (Fig. 1).

Hence, it could be argued that one of the major problems in employing Eq. (1) to ultrathin water films is the treatment of γ as a constant. The dilemma seems solved if one assumes that the force instability in SFM measurements reflects a structural transition of water, i.e., γ changing with RH. Note that the thickness of condensed water vapor films is strongly related to RH, thus a liquid boundary regime at the solid surface could be defined in which water undergoes a structural change. However, this hypothesis is not supported by recent findings. SFG and scanning polarization force microscopy suggest that the force instability is caused by a low coverage of water at the solid surface.[9] We favor this interpretation and will provide further evidence below.

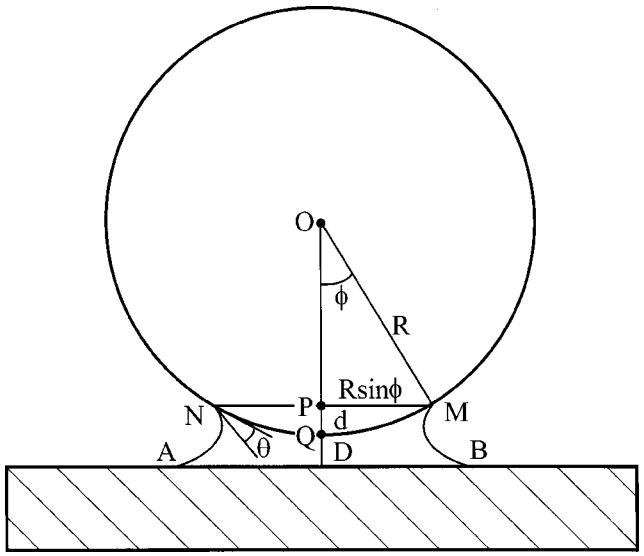

FIG. 2. Sketch of the capillary neck between a sphere and a plane, with R, the radius of the sphere, d, the length of $\overline{PQ}$, D, the distance between the sphere and plane, and ϕ, the angle of $\angle MOP$.

EXPERIMENT

Pull-off force measurements were employed with a modified commercial SFM (EXPLORER from Thermomicroscope Inc.) based on the beam-deflection scheme.[27] The pull-off forces were obtained from SFM force-displacement curves with approaching speeds of 0.5 μm/s to avoid inertial and damping effects. The microscope was situated in a glove box. The RH value inside the chamber was controlled by water evaporation combined with the inlet flow rate of dry nitrogen gas. A thermo-hygrometer (Omega RH83) was used to measure RH with $\pm 4\%$ uncertainty. The temperature in the box was $22\pm 1\,^{\circ}\mathrm{C}$.

For our nanocontact measurements, we chose the following cantilever materials and spring constants: silicon nitride (Si_3N_4), spring constants of 0.032 and 0.064 N/m (Thermomicroscope Inc.), silicon nitride (Si_3N_4), spring constants of 0.1 and 0.5 N/m (Park Instruments), and silicon, spring constant of 0.12 N/m (Nanosensors GmbH). For our microcontact measurements, a silica glass sphere (Duke Scientific Corp.) was glued to the end of a Si_3N_4 cantilever by using a three-dimensional micromanipulation stage and an optical microscope (Wild M420). A flame-drawn glass capillary was used to apply the epoxy. The sphere was then carefully positioned with a second glass capillary. The radius of the glued microsphere was 3.7 μm measured by scanning electron microscopy. The radius of the sphere exceeded that of a typicalcantilever tip (about 10–20 nm) by as much as 100–200 times. Typical cantilever tips and uncoated silica glass spheres are hydrophilic.

To prepare a hydrophobic tip, a cantilever (Digital Instrument, silicon nitride, spring constant 0.12 N/m) was reacted with *n*-octadecyltrichlorosilane (OTS) to produce a covalently bound networked hydrocarbon film on the tip surface. The OTS was deposited at room temperature from a dilute hexadecane/CCl_4/CH_3Cl solution. After reaction, the tip was baked at 120 °C for 2 h to drive the reaction to completion. This procedure produces very smooth films with the thickness of only a few multilayers. The hydrophobic character of the OTS layer was confirmed by a contact angle (advancing) measurement of 105.5°.[28]

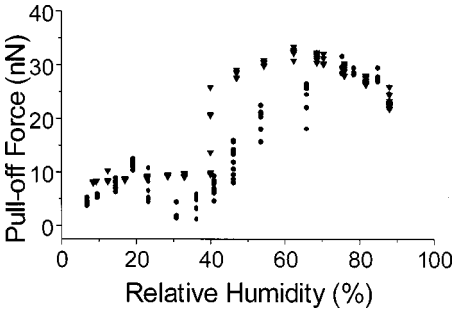

FIG. 3. Pull-off force vs RH measured between a hydrophilic tip and a flat silicon sample. (●) Measured when increasing RH, (▼) measured when decreasing RH.

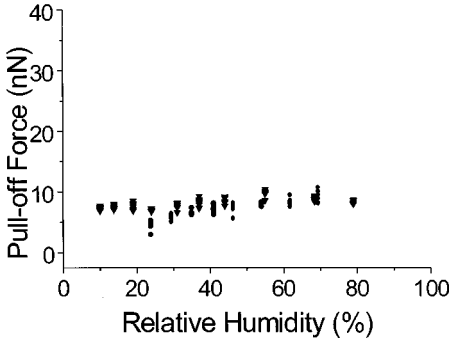

FIG. 5. Pull-off force vs RH measured between a sharp SFM tip coated with OTS and a flat silicon sample. The pull-off force is independent of humidity.

As flat sample surfaces we chose silicon wafers and epitaxially grown (111) calcium fluoride films. Silicon was cleaned prior to the measurements with acetone in an ultrasonic cleaner. Note that these two sample surfaces are also hydrophilic, like the uncoated tips and silica spheres. The solubility of calcium fluoride in water became apparent in force-displacement measurements at higher humidity (see below).

RESULTS AND DISCUSSION

Figure 3 shows the results of pull-off force vs RH measurements conducted with a hydrophilic tip on a silicon sample. At low RH ($\leqslant$40%), the pull-off force is constant. In the mid-RH range ($40\% \leqslant RH \leqslant 70\%$), the pull-off force increases with increasing RH. A pull-off force RH hysteresis is noticeable in this regime. At 40% RH a force discontinuity occurs. The transition seems to be more pronounced for decreasing humidity than for increasing humidity, which is an instrumental artifact due to improved control of RH for decreasing humidity. At RH larger than 70%, the pull-off force decreases with increasing humidity. The RH transition is not affected by the choice of spring constants.

For the silica glass sphere cantilever (microcontact), the pull-off force was observed to increase with RH in the range of 30%–40% (Fig. 4), which was a little lower than the value of 40% RH for the hydrophilic tip.

The transition around 40% RH for hydrophilic contact surfaces qualitatively resembles the results previously obtained on mica surfaces.[6] Strong interactions between water and mica surfaces are expected due to the very polar nature of mica after cleaving. The hypothesis of water structuring (or restructuring) on mica is feasible also because of the crystalline surface structure of mica. However, these two arguments for water structuring on silicon oxide fail due to the amorphous surface structure of silicon oxide.

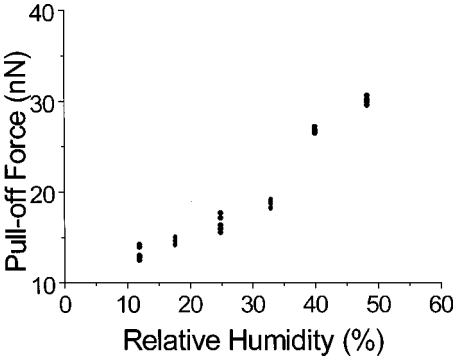

FIG. 4. Pull-off force vs RH measured between a silica glass sphere and a flat silicon sample when increasing RH.

Nevertheless, let us assume that water undergoes a phase change at 40% RH if interfacially confined by a hydrophilic silicon oxide surface. It can be assumed that this structural phase change is independent of any pressure confinement. Otherwise, the transitions of a sharp tip and a blunt microsphere should have occurred at significantly different RH values, which is not reflected in Figs. 3 and 4. The thickness of the water film on the substrate surface depends on RH. Thus, the restructuring transition in water occurs in the close vicinity to the silicon substrate, because the water film is thinning with decreasing humidity. Note that only one hydrophilic surface is necessary to form a water film. Hence, the water restructuring process and its detection in pull-off force measurements should not depend on the cantilever probe material as long as the sample is hydrophilic.

For a hydrophobic tip coated with OTS, on the same silicon substrate as above, we observed constant pull-off forces (that is, independent of RH) in the entire range from 10% to 80% RH (Fig. 5). This does not support the assumption of water structuring at the sample surface, and is consistent with previous pull-off force measurements of hydrophilic tips and hydrophobic surfaces (coated silicon).[12] Hence, the force instability does not originate from a structural phase transition but from the ability or inability of the water film to form a liquid joining neck between the adjacent surfaces at high and low RH, respectively.

Based on the above results, we divided the pull-off force measurements of adjacent hydrophilic surfaces (Fig. 3) into three regimes as illustrated in Fig. 1. In regime I, no capillary neck is developed, and the pull-off force is dominated by van der Waals interactions. A capillary neck is formed at about 40% RH, which corresponds to the force discontinuity observed between regimes I and II. We can understand this transition-like behavior of the pull-off force by considering the minimum thickness requirement of water precursor films for spreading.[29,30] The height of the precursor film cannot drop below a certain minimum, *e*, which is

$$e=a_0\left(\frac{\gamma}{S}\right)^{1/2};\quad a_0=\left(\frac{A}{6\pi\gamma}\right)^{1/2};\quad S=\gamma_{SO}-\gamma_{SL}-\gamma, \qquad (2)$$

where a_0 is a molecular length,[30] S the spreading coefficient, A the Hamaker constant, γ_{SO} the solid–vacuum interfacial energy, and γ_{SL} the solid–liquid interfacial energy.

We propose that the formation of the capillary neck also requires a minimum height of the water film. No capillary neck forms between two surfaces until the water film thickness reaches the minimum thickness. The water film thickness was found to increase with the increase of RH (p/p_s),[20] i.e., the thickness of the water film on the silicon surface is too thin to form a capillary neck with the probing tip for RH less than 40%. When the water film thickness reaches the minimum thickness requirement at 40% RH, a capillary neck forms between the tip and the substrate surfaces, leading to a sudden increase of the pull-off force.

The magnitude of pull-off forces measured on hydrophilic silicon surfaces below 40% RH is $8\pm3\,nN$ (Figs. 3 and 5). For RH larger than the critical RH, in the mid-RH regime II (Figs. 1 and 3), the capillary force dominates the pull-off force if both surfaces are hydrophilic. Thus, the SFM observable—the pull-off force—is not a direct measure of the capillary force only. In regime II the pull-off force can be described as the sum of the capillary force (F_{cap}) and van der Waals interaction force (F_{vdw}):

$$F_{pull}=F_{cap}+F_{vdw}. \qquad (3)$$

In regime I, the pull-off force is restricted to van der Waals interaction between the cantilever tip and the sample surfaces. Both F_{cap} and F_{vdw} are attractive.

In the high RH regime III (Figs. 1 and 3), the pull-off force decreases with increasing RH for a hydrophilic tip. Mate and Binggeli[5] discussed the decrease as the interplay between capillary forces and the forces related to the chemical bonding of the liquid in the gap. This leads to the following expression for the pull-off force:

$$F_{pull}=F_{cap}+F_{vdw}+F_{chem};\qquad F_{chem}=-\frac{\partial G}{\partial z}=-\frac{a}{v}\mu=-\frac{a}{v}kT\ln\left(\frac{p}{p_s}\right), \qquad (4)$$

where F_{chem} (Ref. 5) is the force related to the chemical bonding with G the Gibbs free energy, a the area of the liquid film, v the molar volume, and μ the chemical potential.

Measurements with hydrophilic cantilever tips on ionic surfaces, such as calcium fluoride (CaF_2), show a similar qualitative trend in the pull-off force at low RH (Fig. 6) as found above on silicon surfaces. At intermediate RH, the pull-off force collapses very rapidly with increasing RH. This can be explained by ion-diffusion from calcium fluoride surface into the water film, which has a strong affect on the material properties such as the surface tension.

Roughness effects can explain why force values (Fig. 4) for presumable microcontacts (silica glass sphere) at low loads are significantly smaller than expected from Eq. (1). The roughness of the sphere is 10 nm rms determined from a second-order flattened SFM image over 1 μm^2 area of the sphere surface. At low load, the sphere makes contact with multiple nanosized asperities. This leads to a significant decrease in the pull-off force in the van der Waals interaction regime compared to an atomically smooth sphere. The argument also holds in the capillary regime. The force instability measured with silica glass spheres is widened by the asperity size dispersion, and the magnitude of the pull-off force is determined by the number of asperities in contact. Halsey and Levine suggested that the adhesive force between two rough spheres was dependent on the total amount of the fluid present.[31]

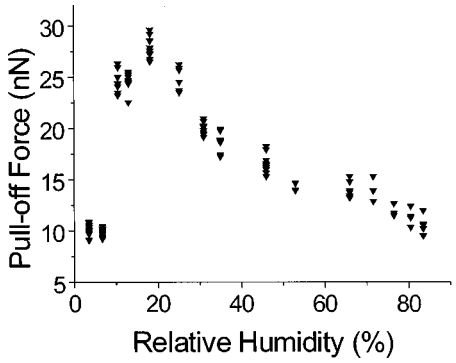

FIG. 6. Pull-off force vs RH measured between a hydrophilic tip and a flat ionic calcium fluoride sample when decreasing RH.

SUMMARY AND CONCLUSION

We critically analyzed SFM pull-off force measurements regarding their applicability to test structural changes in interfacially confined ultrathin fluid films. Pull-off force discontinuities were found on amorphous silicon surfaces and ionic crystal calcium fluoride surfaces. The obtained force discontinuities on silicon surfaces resemble SFM experiments previously obtained on mica surfaces which were interpreted as possible structural transition in interfacially confined water films. Based on our measurements, we conclude that pull-off force measurements conducted with hydrophilic tips are inadequate in determining the nature of the force transition in thin water films.

We divided the force–humidity spectra with hydrophilic interfaces into three regimes; (I) a van der Waals regime at low RH, (II) a capillary force dominated mid-RH regime, and (III) a mixed repulsive-attractive regime at high RH. Regimes I and II are distinguished by a dramatic force discontinuity which reflects the ability or inability of the thin water film to form a capillary neck. The force discontinuity is caused by the minimum thickness requirement of water film to form a capillary neck. When relative humidity is below 20% (calcium fluoride) or 40% (silicon), the water film thickness is too small to form a capillary neck with a hydrophilic tip. At high RH, repulsive forces related to the chemical potential depress overall pull-off forces. Ionic diffusion is expected to be responsible for the significantly lowered RH of force instability found with calcium fluoride. Roughness of the silica glass sphere reduces the magnitude of pull-off forces and the asperity size dispersion widens the force instability profile.

ACKNOWLEDGMENTS

This work was supported by the Petroleum Research Fund administered by the American Chemical Society and by the Shell Foundation's Faculty Career Initiation Fund. Amy Szuchmacher was supported by a grant from the University of Washington Nanotechnology Center.

APPENDIX: CAPILLARY FORCE EQUATION FOR NANOCONTACTS

We derived the capillary force equation for nanocontacts from the sphere–plane approximation, found in Ref. 26, with the distinction that we did not require a large contact area, and thus, do not restrict our capillary force equation to large sphere radii, R (Fig. 2).

Starting from the surface free energy of the system, W,[26]

$$W=-\gamma s+c;\quad s=\pi(d^2+2R^2\sin^2\phi);$$

$$d=R(1-\cos\phi), \tag{A1}$$

where ϕ is the angle of $\angle MOP$, s the wetted surface area, and c a constant. The capillary force can be introduced as

$$F=-\frac{dW}{dD}=\pi R^2\gamma[2\sin\phi(1+\cos\phi)]\frac{d\phi}{dD}, \tag{A2}$$

where D is the distance between the sphere and the plane. The differential term of the angle ϕ with D can be obtained by an isovolume consideration ($dV/dD=0$) of a simplified meniscus volume (*ABMQN*), V, which equals the volume of the cylinder *ABMN* minus the volume of the spherical cap *MNQ*. The simplified meniscus volume is

$$V=\pi R^2\sin^2\phi(D+d)-\frac{\pi R^3}{3}(1-\cos\phi)^2(2+\cos\phi). \tag{A3}$$

Equation (A3) leads to the following relationship:

$$\frac{d\phi}{dD}=\frac{\tan\phi}{2R(1-\cos\phi)\left(1+\dfrac{D}{d}\right)}. \tag{A4}$$

This equation is also applicable to small contacts. The capillary force is derived by substituting Eq. (A4) into Eq. (A2),

$$F=\pi R\gamma\cos\theta\frac{(1+\cos\phi)^2}{\cos\phi\left(1+\dfrac{D}{d}\right)}, \tag{A5}$$

which yields a capillary force at contact ($D=0$),

$$F_{\text{cap}}^{R\sim d}=F_{\max}=\pi R\gamma\cos\theta\frac{(1+\cos\phi)^2}{\cos\phi}. \tag{A6}$$

Equations (1) and (A6) differ by the geometrical factor

$$K=\frac{(1+\cos\phi)^2}{4\cos\phi}, \tag{A7}$$

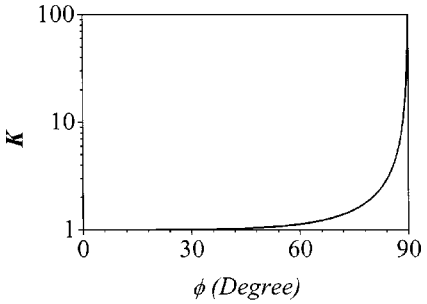

FIG. 7. Relationship between the geometrical correction factor K [Eq. (A7)] and the angle ϕ (Fig. 2).

which is important for small asperity contacts, i.e., large angles of ϕ (Fig. 7). Equation (1) can be applied with a 20% uncertainty for an angle ϕ of less than 70°.

Yang and co-workers observed large pull-off forces (i.e., 100–200 nN) on mica with typical hydrophilic cantilever tips,[14] which we propose to explain with a large K factor.

Note that Eq. (A6) is based on a very simplified cylindrically shaped geometry. More sophisticated geometries are found in the literature for macrocontacts or microcontacts,[5,21–24] and for nanocontacts.[32]

[1] E. Barthel, X. Y. Lin, and J. L. Loubet, J. Colloid Interface Sci. **177**, 401 (1996).
[2] J. Crassous, E. Charlaix, and J. L. Loubet, Phys. Rev. Lett. **78**, 2425 (1997).
[3] L. R. Fisher and J. N. Israelachvili, J. Colloid Interface Sci. **80**, 528 (1981).
[4] L. R. Fisher and J. N. Israelachvili, Colloids Surface **3**, 303 (1981).
[5] M. Binggeli and C. M. Mate, Appl. Phys. Lett. **65**, 415 (1994).
[6] L. Xu, A. Lio, J. Hu, D. F. Ogletree, and M. Salmeron, J. Phys. Chem. B **102**, 540 (1998).
[7] J. Hu, X.-D. Xiao, D. F. Ogletree, and M. Salmeron, Science **268**, 267 (1995).
[8] J. Hu, X.-D. Xiao, and M. Salmeron, Appl. Phys. Lett. **67**, 476 (1995).
[9] P. B. Miranda, L. Xu, Y. R. Shen, and M. Salmeron, Phys. Rev. Lett. **81**, 5876 (1998).
[10] T. Thundat, X.-Y. Zheng, G. Y. Chen, and R. J. Warmack, Surf. Sci. Lett. **294**, L939 (1993).
[11] T. Thundat, R. J. Warmack, D. P. Allison, L. A. Bottomley, A. J. Lourenco, and T. L. Ferrell, J. Vac. Sci. Technol. A **10**, 630 (1992).
[12] M. Fujihira, D. Aoki, Y. Okabe, H. Takano, and H. Hokari, Chem. Lett. **7**, 499 (1996).
[13] M. Odelius, M. Bernasconi, and M. Parrinello, Phys. Rev. Lett. **78**, 2855 (1997).
[14] G. L. Yang, J. P. Vesenka, and C. J. Bustamante, Scanning **18**, 344 (1996).
[15] A. Schumacher, N. Kruse, R. Prins, E. Meyer, R. Luthi, L. Howald, H. J. Guntherodt, and L. Scandella, J. Vac. Sci. Technol. B **14**, 1264 (1996).
[16] Y. Sugawara, M. Ohta, T. Konishi, S. Morita, M. Suruki, and Y. Enomoto, Wear **168**, 13 (1993).
[17] A. L. Weisenhorn, P. K. Hansma, T. R. Albrecht, and C. F. Quate, Appl. Phys. Lett. **54**, 2651 (1989).
[18] B. V. Derjaguin and N. V. Churaev, J. Colloid Interface Sci. **49**, 249 (1974).
[19] R. M. Pashley, J. Colloid Interface Sci. **78**, 246 (1980).
[20] D. Beaglehole and H. K. Christenson, J. Phys. Chem. **96**, 3395 (1992).
[21] W. C. Clark, J. M. Haynes, and G. Mason, Chem. Eng. Sci. **23**, 810 (1968).
[22] F. M. Orr, L. E. Scriven, and A. P. Rivas, J. Fluid Mech. **67**, 723 (1975).
[23] R. Aveyard, J. H. Clint, and D. Nees, J. Chem. Soc., Faraday Trans. **93**, 4409 (1997).
[24] A. W. Adamson, *Physical Chemistry of Surfaces* (Wiley, New York, 1990).

[25] E. A. Vogler, Adv. Colloid Interface Sci. **74**, 69 (1998).
[26] J. N. Israelachvili, *Intermolecular and Surface Forces*, 2nd ed. (Academic, London, 1992).
[27] G. Meyer and N. M. Amer, Appl. Phys. Lett. **56**, 2100 (1990).
[28] R. Luginbühl, A. Szuchmacher, M. D. Garrison, J. B. Lhoest, R. M. Overney, and B. D. Ratner, Ultramicroscopy **82**, 171 (2000).
[29] R. Bruinsma, Macromolecules **23**, 276 (1990).
[30] P. G. de Gennes, Rev. Mod. Phys. **57**, 827 (1985).
[31] T. Halsey and A. Levine, Phys. Rev. Lett. **80**, 3141 (1998).
[32] A. Marmur, Langmuir **9**, 1922 (1993).